Journal of Crystal Growth 313 (2010) 68–80

Contents lists available at ScienceDirect

Journal of Crystal Growth

journal homepage: www.elsevier.com/locate/jcrysgro

Enhanced growth of methane–propane clathrate hydrate crystals with sodium dodecyl sulfate, sodium tetradecyl sulfate, and sodium hexadecyl sulfate surfactants

Jeffry Yoslim [a], Praveen Linga [b], Peter Englezos [a,*]

[a] Department of Chemical and Biological Engineering, University of British Columbia, 2360 East Mall, Vancouver, British Columbia, Canada V6T 1Z3
[b] Department of Chemical and Biomolecular Engineering, National University of Singapore, 4 Engineering Drive 4, Singapore 117576, Singapore

ARTICLE INFO

Article history:
Received 9 April 2010
Received in revised form
20 September 2010
Accepted 7 October 2010
Communicated by S.R. Qiu
Available online 21 October 2010

Keywords:
A1. Crystal morphology
B1. Gas hydrates
A1. Dendrites
A1. Interfaces
A2. Growth from solutions

ABSTRACT

In the present study the effect of three commercially available anionic surfactants on the hydrate growth from a gas mixture of 90.5 mol% methane/9.5 mol% propane mixture was investigated. The surfactants used were sodium dodecyl sulfate (SDS), sodium tetradecyl sulfate (STS), and sodium hexadecyl sulfate (SHS). The morphology of the growing crystals and the gas consumption were observed during the experiments. The results showed that in the presence of surfactants, branches of porous fibre-like crystals were formed instead of dendritic crystals formed in the absence of any additive. In addition, extensive hydrate crystal growth on the crystallizer walls and a "mushy" hydrate layer instead of a thin crystal film appeared at the gas/water interface. Finally, the addition of SDS with concentration range between 242 and 2200 ppm (ΔT=13.1 K) was found to increase the mole consumption for hydrate formation by approximately 14 times compared to pure water. This increase is related to the change in hydrate morphology, whereby a more porous hydrate forms with enhanced water/gas contacts.

1. Introduction

The addition of surface active agents (surfactants) to water is known to enhance the rate of gas uptake during clathrate hydrate crystallization without affecting the equilibrium formation conditions [1]. The fact that one may enhance the hydrate crystallization rate based on the use of chemical additives has potential practical applications including conversion of natural gas into solid hydrate for storage and transport as a solid natural gas hydrate (NGH) [2–9].

Karaaslan and Parlaktuna [10] found that the addition of the anionic surfactant (linear alkyl benzene sulfonic acid) enhanced the rate of natural gas hydrate formation more than the nonionic (nonylphenol ethoxalate) and the cationic (quaternary ammonium salt). Sun et al. [11] confirmed that an anionic surfactant (sodium dodecyl sulfate) is more effective compared to a nonionic (dodecyl polysaccharide glycoside) in terms of rate of hydrate formation from a methane/ethane/propane mixture. Link et al. [12] concluded that Sodium Dodecyl Sulfate (SDS) is one of the best surfactants commercially available to be used for the enhancement of methane hydrate formation. Okutani et al. [13] found that SDS enhances the rate of difluoromethane (HFC-32) hydrate formation and the water to hydrate conversion. Daimaru et al. [14] carried out hydrate formation experiments in batch-mode and tested three surfactants with sodium sulfonic acid groups but with different carbon chain length (C4, C12, and C18). They observed that methane hydrate formation was five times faster than for pure water at surfactant concentrations up to a certain level. It was also found that Sodium Butyl Sulfate (C4) gave the highest acceleration compared to those with twelve (C12) and eighteen (C18) carbon atoms. Okutani et al. [5] formed methane hydrate in an unstirred chamber in the presence of SDS, sodium tetradecyl sulfate (STS), and sodium exadecyl sulfate (SHS). It was found that SDS, which has the shortest chain length and highest solubility in water increases the rate of hydrate formation to the same extent as STS but at a much higher concentration (1000 versus 100 ppm). SHS which has the longest chain length and lowest solubility was found to be less effective in increasing the rate of hydrate formation.

The promoting effect of SDS is possibly due to the adsorption of the surfactant on the hydrate crystals [15,16]. Zhang et al. [17] investigated the relationship between SDS adsorption and tetrahydrofuran hydrate formation based on zeta-potential and pyrene fluorescence measurements at the hydrate/liquid interface. They concluded that the short induction time of tetrahydrofuran (THF) hydrate formation is due to the adsorption of SDS^- at the hydrate/water (head groups orient towards the hydrate surface and tails towards the aqueous phase) [17]. The competition between the DS^- anion and the bicarbonate ion (HCO_3^-) for adsorption sites was also discussed. Lo et al. [18] studied cyclopropane (CP) clathrate

* Corresponding author. Tel: +1 604 822 6184; fax: +1 604 822 6003.
E-mail address: englezos@interchange.ubc.ca (P. Englezos).

0022-0248/$ - see front matter © 2010 Elsevier B.V. All rights reserved.
doi:10.1016/j.jcrysgro.2010.10.009

hydrate and tetrabutylammonium bromide (TBAB) semi-clathrate hydrate formation in the presence of SDS. Based on zeta potential and pyrene fluorescence measurements, Lo et al. [18] discussed the adsorption of SDS on the hydrate surface and reported that hydrogen bonding between the headgroups of DS^- and the hydrate surface is stronger than the hydrophobic force between the tails of DS^- and the hydrate surface.

According to the systematic review of the literature by Okutani et al. [5], the first mechanism of hydrate growth when surfactant is present in the system was proposed by Kutergin et al. [19] and Mel'nikov et al. [20] They reported that addition of surfactant to liquid water enables the gas/water contact to be maintained until most of the water is converted to hydrate by changing the morphology of the hydrate crystals. Morphology is concerned with the observation of shapes and sizes of forming hydrate boundaries, whose length scales are much larger than molecular structure and much smaller than system dimension [21]. Okutani et al. [5] reported observations on macroscopic hydrate-phase growth and concluded that it is in qualitative agreement with the literature, which suggests that capillary-driven water suction that allows water to flow upward through the porous hydrate layer is responsible for enhanced hydrate formation when surfactant is present in the system [6,19,20,22–24]. Okutani et al. [5] also reported that there is no distinct qualitative difference in hydrate growth behaviour with various surfactant types with different alkyl chain lengths and the surfactant concentration used (~100–4000 ppm). Tajima et al. [25] formed hydrates of chlorodifluoromethane (HCFC-22) in a static mixer and observed the formation process through a glass tube. They concluded that the morphology of hydrates was different in the presence of SDS at concentrations above 250 ppm.

Morphological observations have been employed in our laboratory to enable a mechanistic understanding of hydrate formation at various interfaces, which revealed the porous nature of hydrate layers surrounding water droplets and the transport of water through them in agreement with similar reports of water permeation through hydrates [26–29]. Lee et al. [21] examined morphology of methane–propane–water system without addition of any additives and found that hydrates started to form as a thin film at the gas/liquid interface. Hydrate crystals are then observed to grow downwards as dendrites from the thin film into the bulk water. Kumar et al. [30] examined the morphology of the hydrate formed by a methane/propane gas mixture in the presence of poly vinylpyrrolidone (PVP), which is known to inhibit hydrate growth. They observed whiskery type of hydrate crystals at an undercooling of 13.7 K and fibre-type growth at 8.1 K of undercooling. The inhibitor altered the morphology of the hydrate crystals in a manner that depended on the PVP concentration. It was found that at 1.0 wt%, most water molecules initially in liquid phase is converted into hydrate, because the transport barrier provided by the hydrate film at the gas/liquid interface was absent.

The objective of this study is to further investigate the effect of three commercially available anionic surfactants (SDS, STS, and SHS) on the growth characteristics of methane/propane hydrate crystals by observing the morphology of the growing crystals. The observed behaviour is compared to the behaviour in the absence of any chemical (pure water). The effect of sodium alkyl sulfate (C12) concentration and the degree of under-cooling on hydrate crystal growth is investigated.

2. Experimental section

2.1. Materials

The gas used for the present study was a methane/propane (90.5/9.5 mol%) mixture (Praxair Technology Inc.). This composition was chosen in order to simulate natural gas light hydrocarbons; lower operating conditions, and also it is noted that this gas mixture forms structure II. Three anionic surfactants were used: Sodium Dodecyl Sulfate (SDS), Sodium Tetradecyl Sulfate (STS), and Sodium Hexadecyl Sulfate (SHS).

2.2. Apparatus and procedure

The apparatus of Lee et al. [21] was used but was modified by installing a digital pressure transmitter (Rosemont) coupled with a data acquisition system (National Instruments) and a computer with Labview 8.1 software. Briefly, the apparatus consists of a crystallizer (50 cm^3) immersed in a temperature controlled water bath. Two microscopes were used during the experiments, where each of them has a different purpose. A Nikon SMZ-2T microscope attached with a Nikon D-40 was used to capture the system dimension images. The lens used was 0.5 × auxilary lens. The

Table 1
Experimental conditions, surfactant concentration and results.

Experiment number	Surfactant concentration (ppm)	Pressure (kPa)	Temp Eq. (K)	Formation (K)	ΔT (K)	Pressure drop (kPa)
A-1	Water	3200	288.7	275.6	13.1	58.5
A-2	Water	3200	288.7	275.6	13.1	44.7
B-1	SDS-2200	3200	288.7	275.6	13.1	837.6
B-2	SDS-2200	3200	288.7	275.6	13.1	796.2
B-3	SDS-2200	3200	288.7	275.6	13.1	754.8
C-1	SDS-2200	2400	286.4	278.4	8	446.7
C-2	SDS-2200	2400	286.4	278.4	8	432.9
C-3	SDS-2200	2400	286.4	278.4	8	439.8
D-1	SDS-2200	1430	282.0	278.4	3.6	146.1
D-2	SDS-2200	1430	282.0	278.4	3.6	139.1
D-3	SDS-2200	1430	282.0	278.4	3.6	125.4
E-1	SDS-645	3200	288.7	275.6	13.1	830.6
E-2	SDS-645	3200	288.7	275.6	13.1	754.8
E-3	SDS-645	3200	288.7	275.6	13.1	734.1
F-1	SDS-242	3200	288.7	275.6	13.1	782.5
F-2	SDS-242	3200	288.7	275.6	13.1	754.8
F-3	SDS-242	3200	288.7	275.6	13.1	637.6
G-1	STS-300	3200	288.7	275.6	13.1	823.8
G-2	STS-300	3200	288.7	275.6	13.1	768.7
G-3	STS-300	3200	288.7	275.6	13.1	706.5
H-1	SHS-40	3200	288.7	275.6	13.1	775.5
H-2	SHS-40	3200	288.7	275.6	13.1	699.6
H-3	SHS-40	3200	288.7	275.6	13.1	678.9

Alphabets in the experiment number represent different experiment, while the number following the alphabet represents the experiment conducted after the elimination of memory.

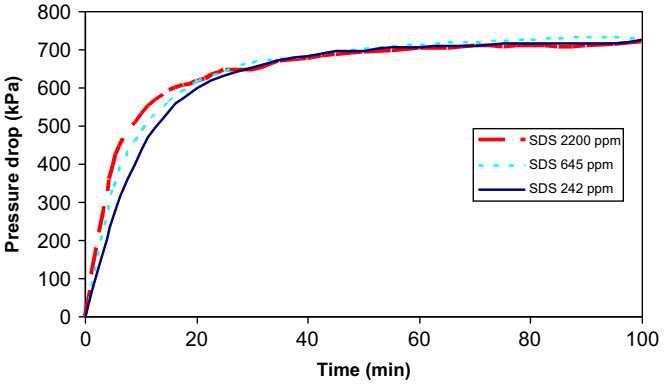

Fig. 1. Pressure drop evolution with time during experiments with three different surfactant concentrations. The experiments were conducted at the same temperature and initial pressure.

second microscope (Nikon SMZ 1000) was used to observe magnified images of hydrate crystals during hydrate formation. These images were saved to the computer with help of CCD camera (Sony, DXC 390). The lens used was P Plan APo 1 × objectives lens. The procedure to conduct the experiments is similar to the one reported by Lee et al.[21] and Kumar et al. [30] The experimental conditions and surfactant type and concentrations are summarized in Table 1. Briefly, 25 cm^3 of aqueous (distilled–deionized water) surfactant solution was injected into the crystallizer. The crystallizer was then pressurized/depressurized thrice with the hydrate forming gas to remove any air present in the crystallizer. The methane/propane gas mixture was fed until the desired experimental pressure was reached. The growth of hydrate crystals was monitored and recorded through the microscope coupled with the CCD Camera. This experiment is denoted as A-1 in Table 1. The hydrate crystals grown in the crystallizer were dissociated by increasing the temperature approximately 3 K above the equilibrium temperature to prepare the next experiment. The time required for the complete dissociation of the hydrates was approximately 60 min This aqueous solution that experienced hydrate formation was used for subsequent morphological experiments as described in Table 1 as A-2 and so on. The stand by time between each formation experiment for a given concentration is 120 min after decomposition [31].

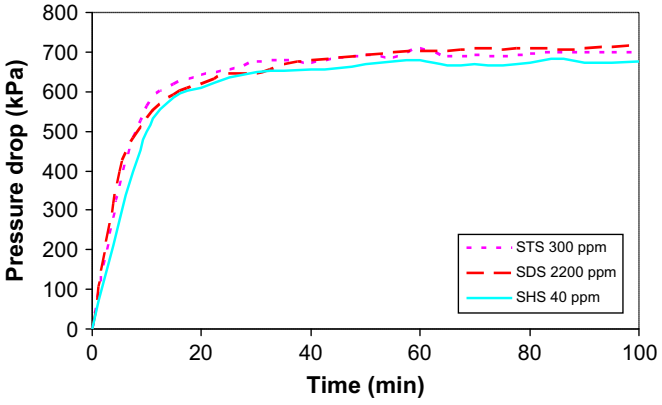

Fig. 2. Pressure drop evolution with time during experiments with three different surfactants. The experiments were conducted at the same temperature and initial pressure.

The concentration of SDS was chosen to be 2200, 645, and 242 ppm (part per million), which are all below the CMC (critical micelle concentration) [9,32]. These three different concentration were chosen because 2200 ppm was the concentration that gave the lowest surface tension [22], the highest storage capacity [33] can be obtained when the concentration was 645 ppm, and the critical micellar concentration (CMC) according to Zhong and Rogers [6] was found to be 242 ppm. The concentrations of SHS and STS were chosen to be 300 and 40 ppm, respectively, since it was reported to have the lowest surface tension [22]. Equilibrium pressure and temperature were calculated using CSMHYD software [34].

3. Result and discussion

The observed pressure drop data due to hydrate formation are summarized in Table 1. These data show that in the presence of surfactant and for any given driving force (under-cooling), the pressure drop due to hydrate formation is significantly higher compared to hydrate formation in the absence of surfactant. In general, the gas consumption in the presence of surfactants was found to be about 14 times higher compared to pure water. Fig. 1 shows the observed pressure drop versus time when SDS is present at different concentrations. As seen there is no significant difference in the total moles of gas consumed as also reported by Okutani et al. [5] for methane hydrate formation. However, the dynamics are different. The experiment with the highest SDS concentration

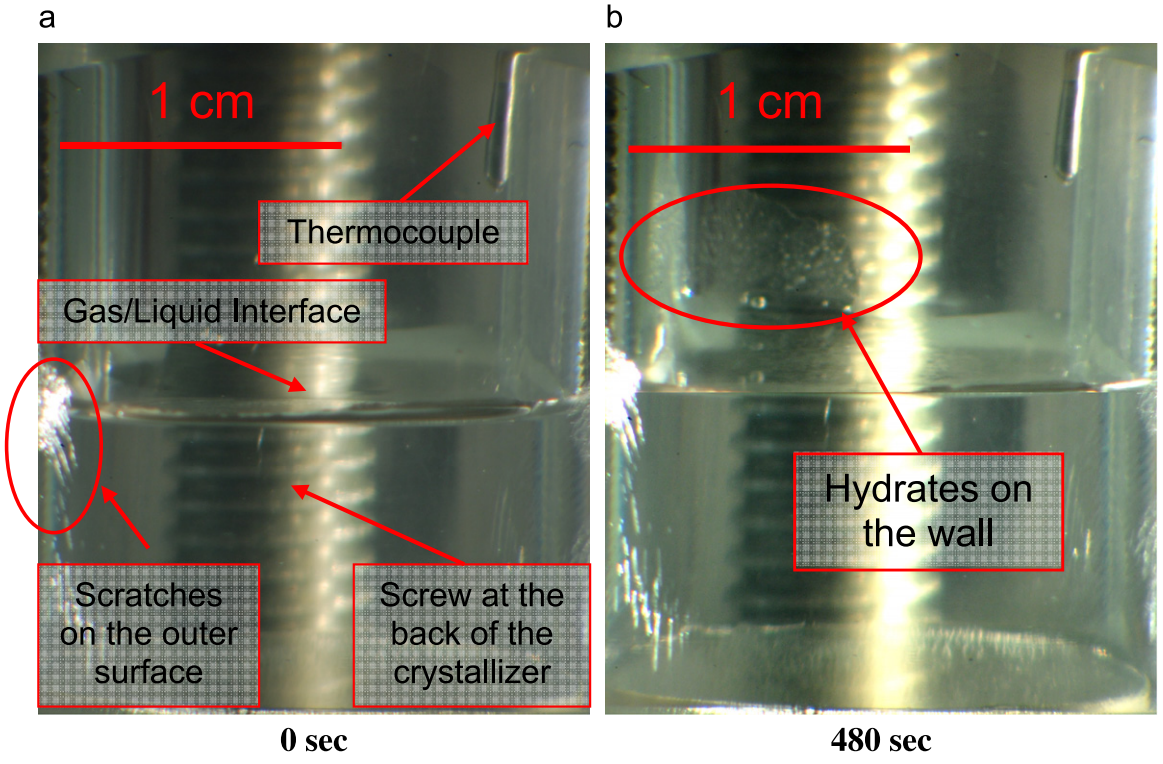

Fig. 3. First growth of hydrate crystals at $\Delta T = 13.1$ K, (Experiment G-3), and without thermocouple present in the liquid phase. The time lapse after the formation started is indicated below each image.

exhibits a steeper pressure drop profile, which indicates a faster rate of hydrate formation. The addition of SDS 2200 ppm was found to decrease the contact angle of the aqueous solution on the Lexan surface from 41° to 29° [31]. It is not clear whether this correlates with the enhanced rate of hydrate formation. The procedure for contact angle measurement is available in the literature [31,35]. Fig. 2 shows similar data but with the three different surfactants. As seen there is no significant difference between the three systems in

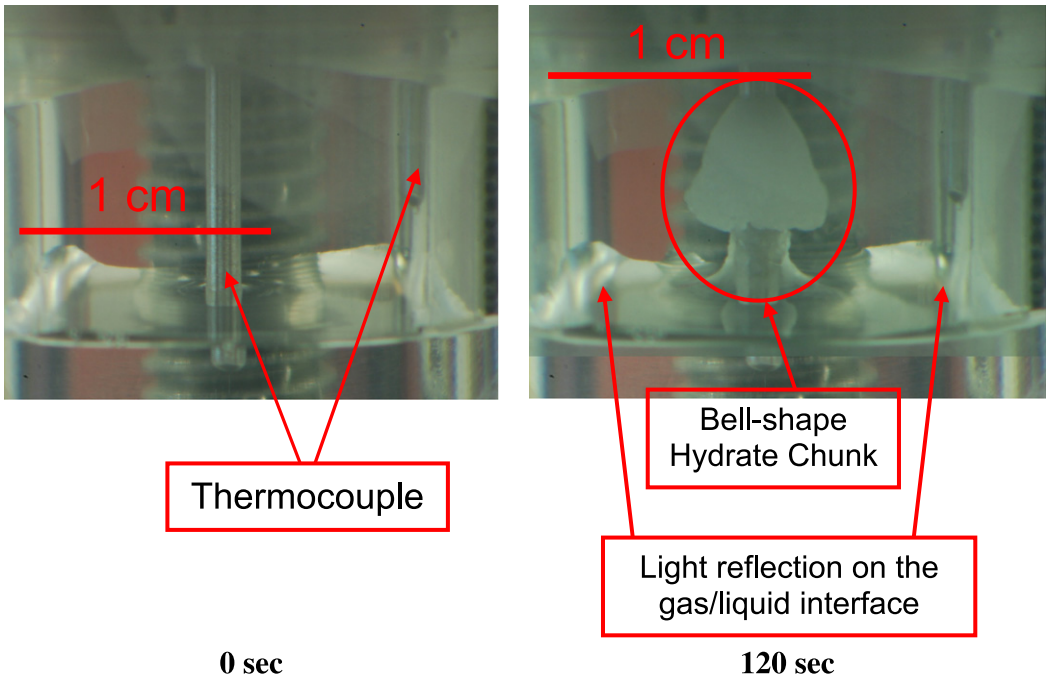

Fig. 4. First growth of hydrate crystals at $\Delta T = 13.1$ K, (Experiment G-2), and with thermocouple present in the liquid phase. The time lapse after the formation started is indicated below each image.

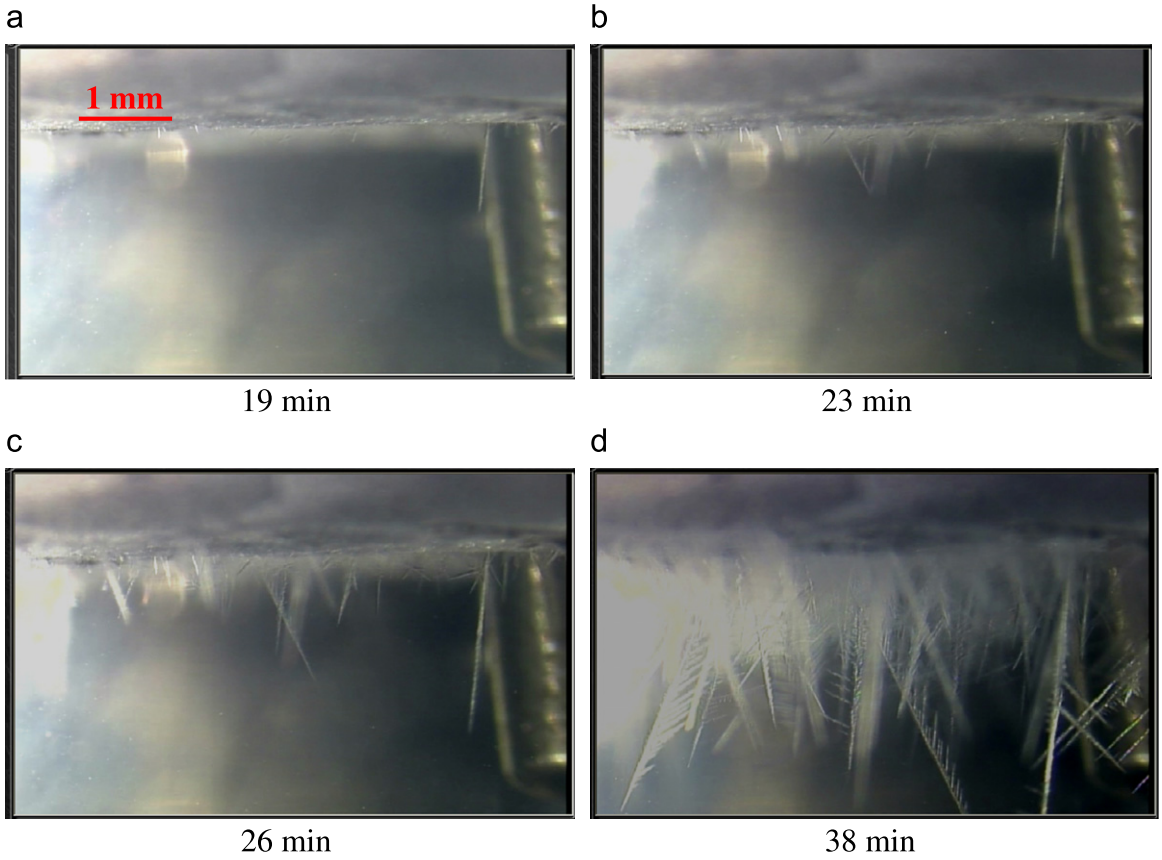

Fig. 5. Sequential images of methane–propane hydrate crystals formed in water (Experiment A-1). The time lapse after hydrate formation is indicated below each image.

terms of the rate of hydrate formation and final pressure drop or gas consumed. This indicates that the surfactants have the same effect albeit at different concentrations. The results above confirm previous findings that surfactant addition enhances the gas uptake. This translates to enhanced hydrate growth. Fig. 3 shows the preferred location of hydrate nucleation is the wall of the crystallizer just above the gas liquid/gas/solid (Lexan) line. However, when a thermocouple is present in the liquid phase the preferred nucleation site is the circumference of the thermocouple (solid/liquid/gas line) as shown in Fig. 4. It is noted that without additives in the system, hydrates start to grow at the gas/water interface as a thin film and cover the entire gas/water interface within 30 s. Subsequently, needle-like hydrate crystals are observed to grow in the downward direction from the thin film into the bulk water as illustrated in Fig. 5 and is in agreement with that reported by Lee et al. [21] and theoretical expectations as a phase change process.

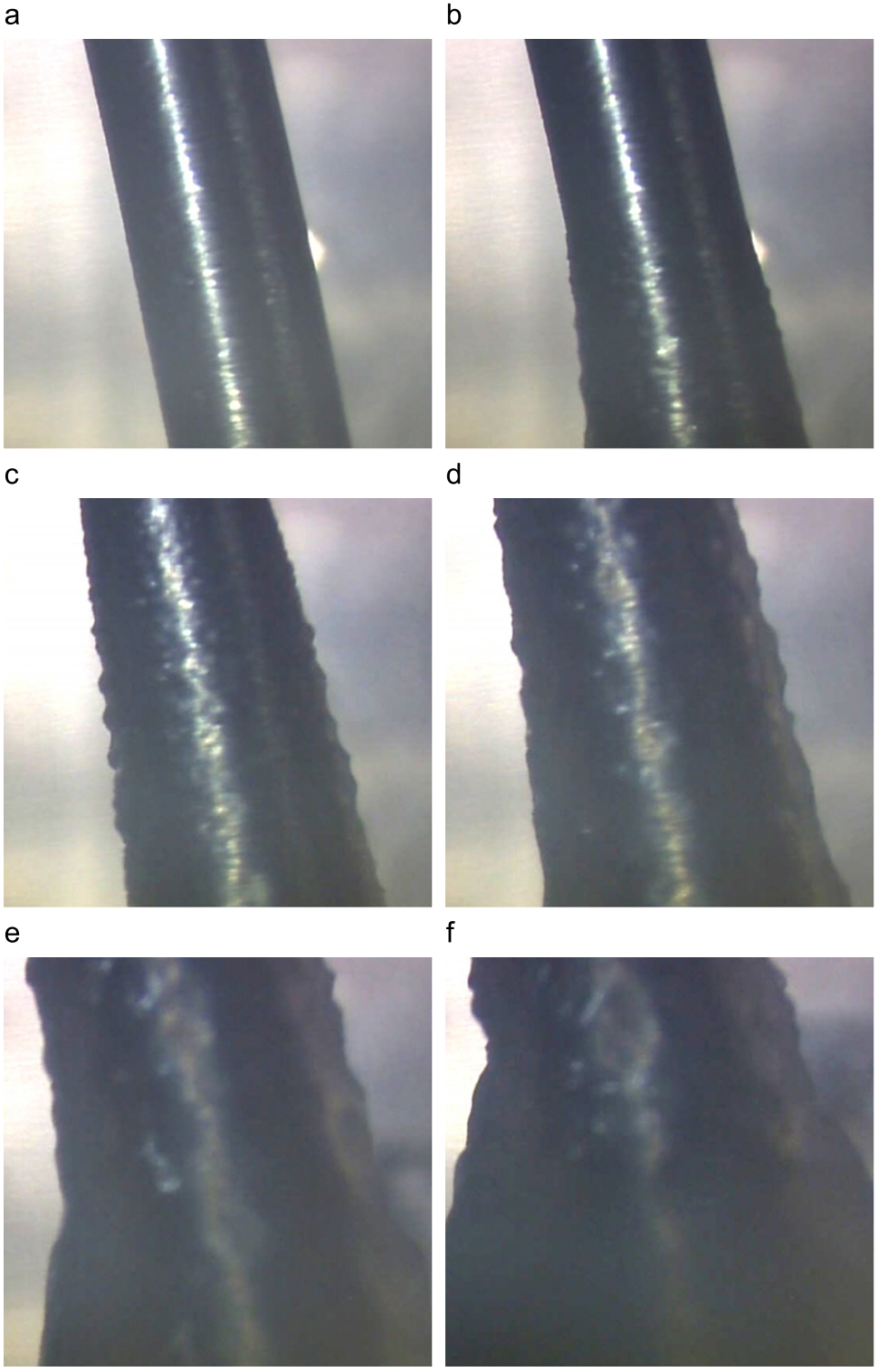

Fig. 6. Hydrate growth on the thermocouple body (Experiment G-2): (a) 0 sec, (b) 15 sec, (c) 25 sec, (d) 35 sec, (e) 45 sec, and (f) 50 sec.

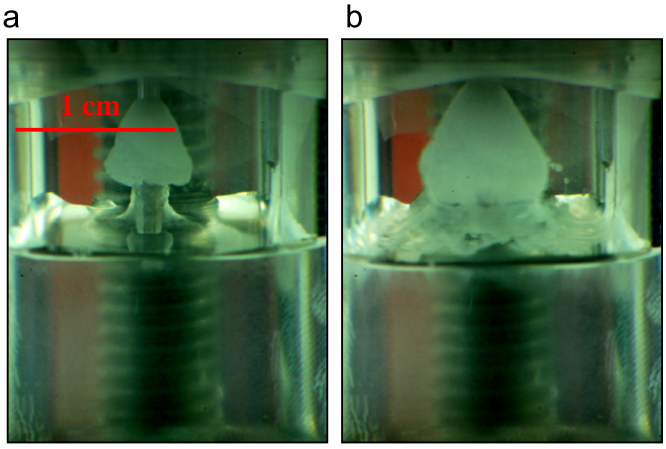

Fig. 7. Mushy hydrate growth in the gas/water interface (Experiment G-2): (a) 120 sec and (b) 180 sec.

In Fig. 4, hydrates can be seen to grow along the circumference of the thermocouple part that is located just above the liquid solution but no hydrates can be seen to grow on the crystallizer wall yet. This phenomenon confirms that the stainless steel (thermocouple)/water interface is a preferred location for hydrate nucleation compared to the crystallizer wall made from Lexan. Perhaps this is due to the fact that the metal surface is a more effective material for heat removal or a preferred site for heterogeneous nucleation. The magnified images of the thermocouple body during hydrate formation are shown in Fig. 6 to give a better illustration of the growth of the hydrate crystal chunk. These series of images show that bulky hydrate layer started to form at the water/gas/thermocouple line and then grew upward at a rate faster than its growth to the sides. The focus of these images is ~1–2 mm above the gas/water interface and the time corresponding to the images is indicated below each image.

In addition, the image on the right side of Fig. 7 also shows a bell-shaped hydrate crystal chunk to grow along the thermocouple body above the liquid solution. The bell-shaped hydrate chunk indicates that

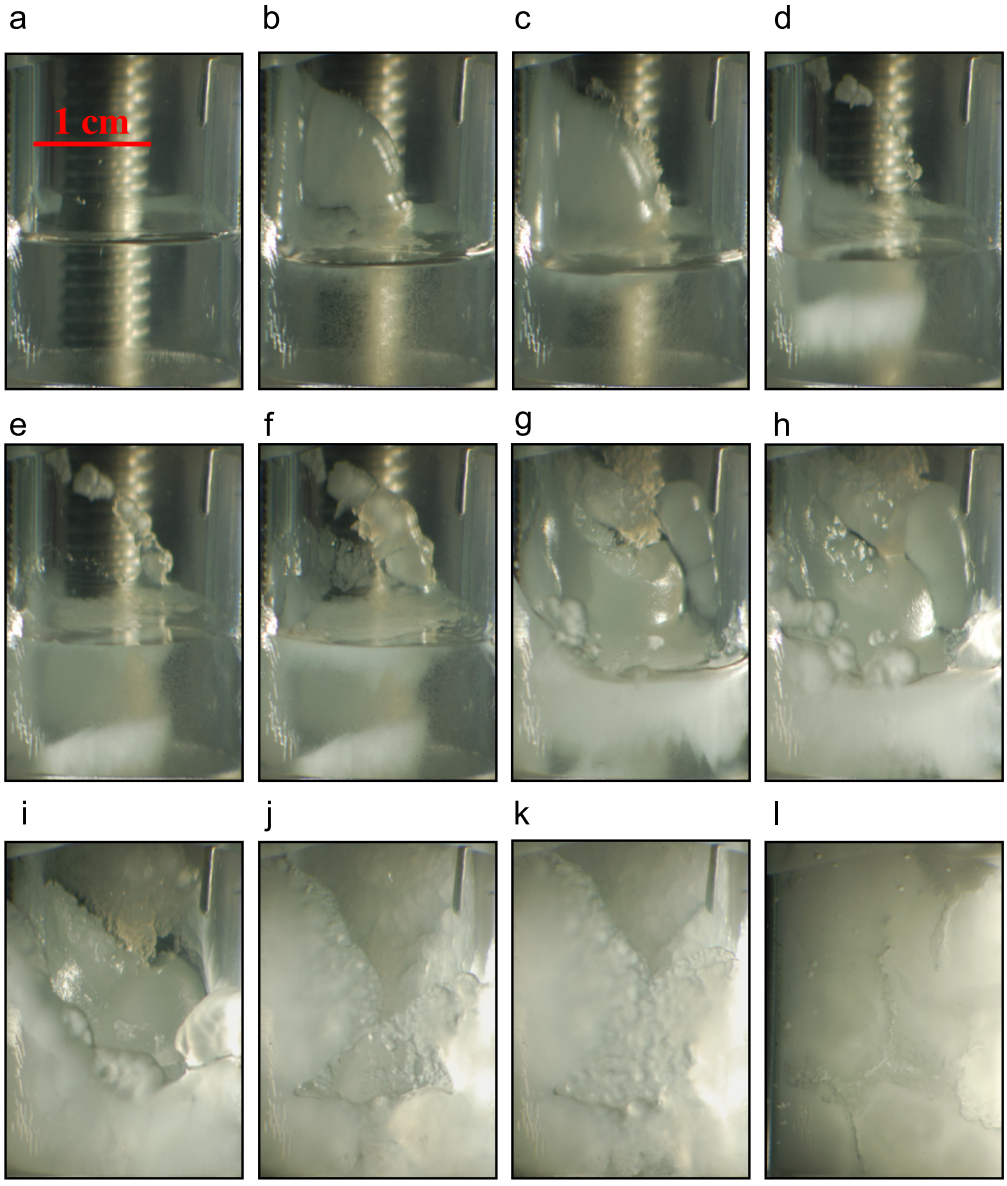

Fig. 8. Sequential images of hydrate crystals from hydrate formation without a thermocouple in the water phase (Experiment G-3). Bulky hydrate formed on the wall eventually falls in the liquid water pool: (a) 0 sec, (b) 480 sec, (c) 540 sec, (d) 560 sec, (e) 580 sec, (f) 600 sec, (g) 660 sec, (h) 690 sec, (i) 720 sec, (j) 840 sec, (k) 900 sec, and (l) 1800 sec.

hydrate growth on the thermocouple is not only vertical (upward) but also horizontal (the chunk gets thicker). Following nucleation, hydrate was also seen to grow radially to cover the gas/liquid water interface as shown in Fig. 7. These hydrate crystals on the gas/liquid water interface started from the base of the hydrate chunk on the thermocouple body and grew to cover the entire gas/liquid water interface. The hydrate layer on the water/gas interface and the hydrate layers on the wall continued to grow upwards. The observations discussed so far are also valid for SDS and SHS provided that the driving force/degree of undercooling is the same (Experiments B, E, F, G, and H).

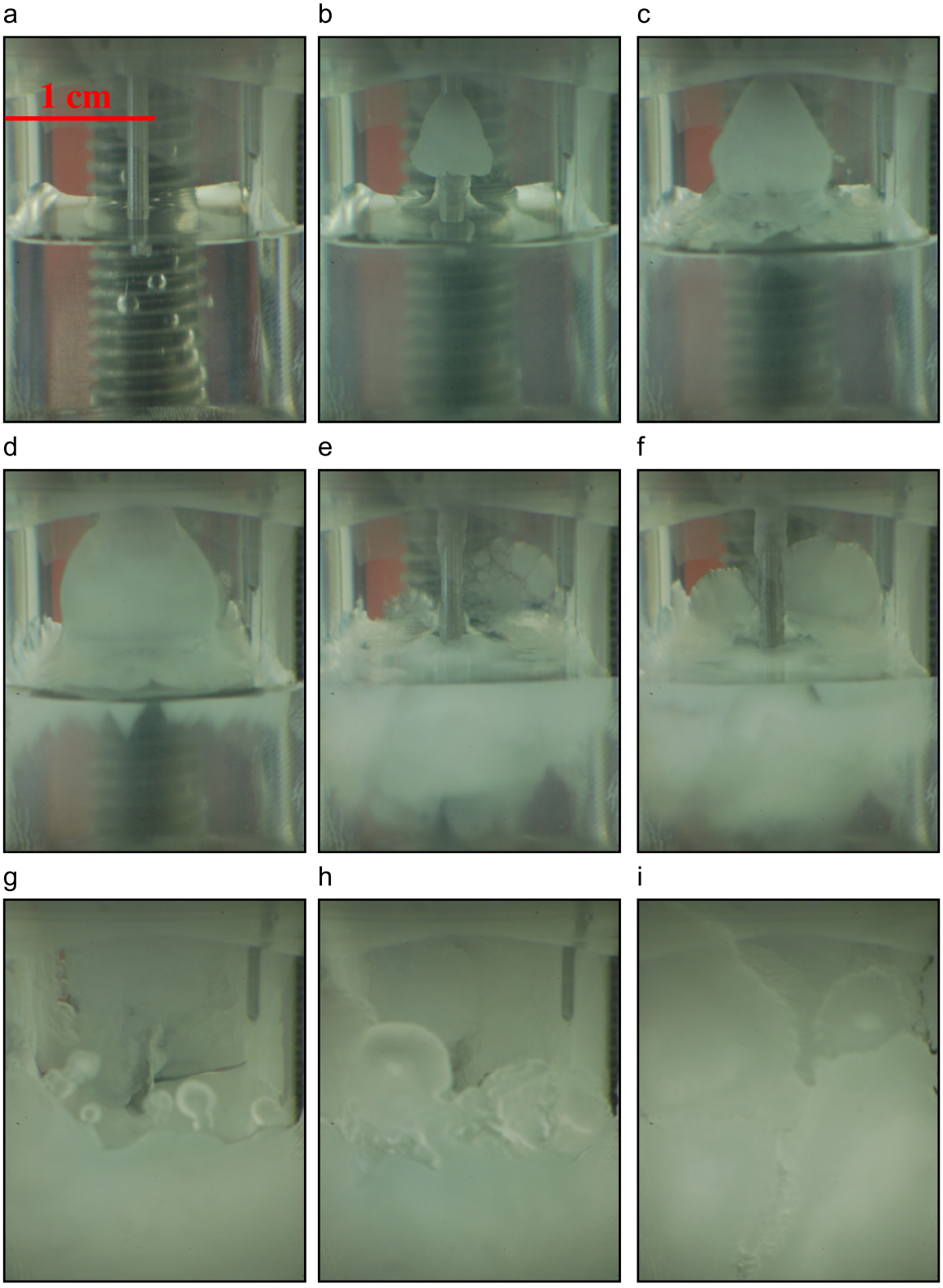

Fig. 9. Sequential images of hydrate crystals from hydrate formation with a thermocouple in the water phase (Experiment G-2). Bulky hydrate layer formed on the wall and/or thermocouple body falls into the liquid pool: (a) 0 sec, (b) 120 sec, (c) 180 sec, (d) 200 sec, (e) 210 sec, (f) 240 sec, (g) 360 sec, (h) 420 sec, and (i) 1800 sec

Figs. 8 and 9 show two typical series of hydrate formation process using a 25 ml aqueous solution containing 300 ppm of STS. In Fig. 8, no thermocouple in the liquid phase is installed. Fig. 9 shows the macroscopic hydrate-phase growth when a thermocouple is present in the liquid phase. It is also noted from Figs. 8 and 9 that the hydrate layers along the crystallizer wall consist of fine

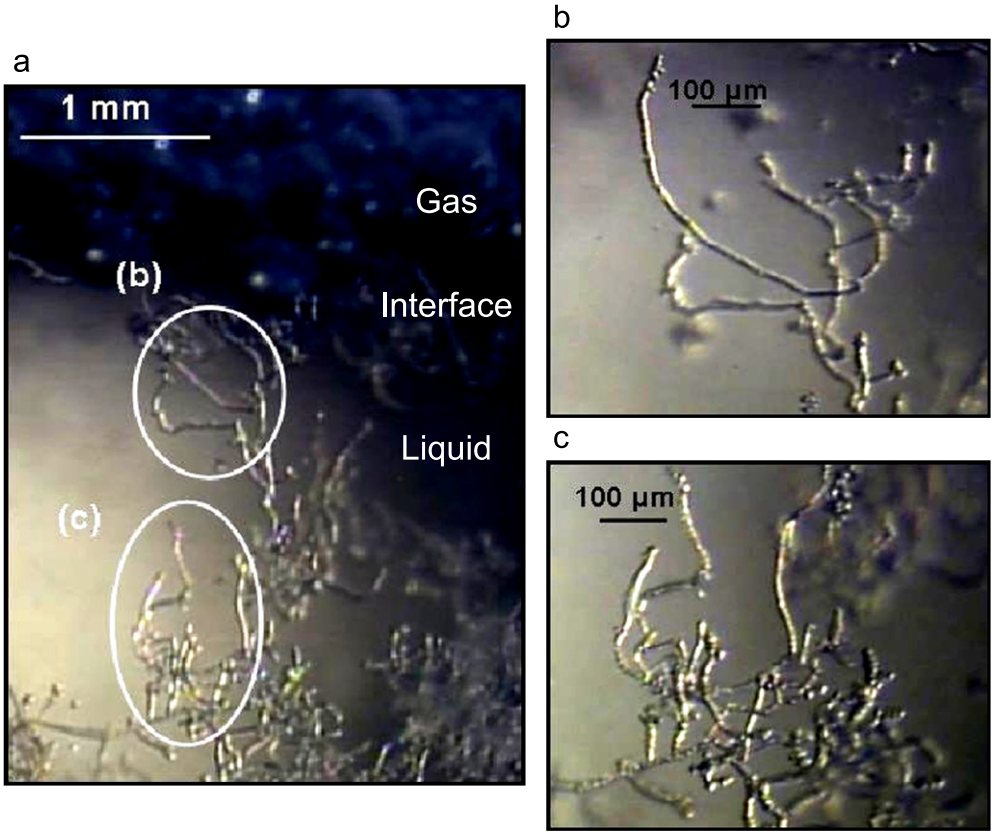

Fig. 10. Images of branched fibre-like hydrate crystals formed with surfactant present in the system (Experiment C-1). Image (b) and (c) are magnified images from (a).

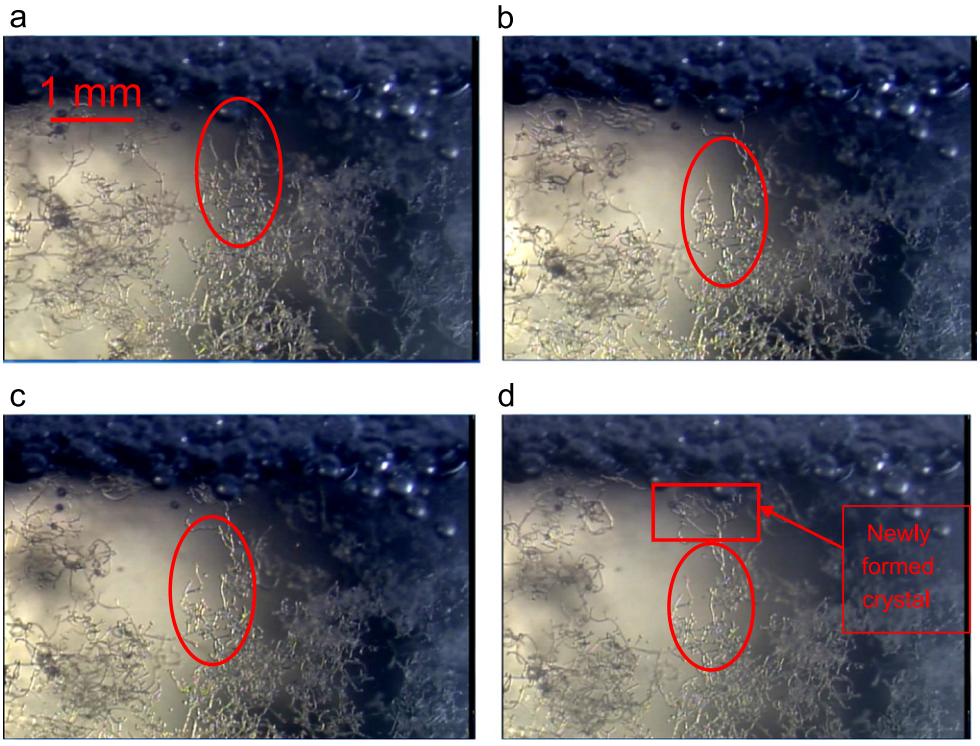

Fig. 11. Growth of fibre-like crystals (Experiment C-1): (a) 26 min and 44 sec, (b) 27 min and 24 sec, (c) 27 min and 44 sec, and (d) 28 min and 4 sec.

fibre-like crystals (540 and 560 s images from Fig. 8, and 200 and 210 s images from Fig. 9). The bulky hydrate layer on the wall and/or thermocouple body falls into the liquid pool once it gets heavier and the water level decreases so that there is less support from the bottom. Once the bulky hydrate chunk drops back to the liquid pool, it leaves a wet surface on the wall that will quickly form hydrate again. In this apparatus, a hydrate layer continued to grow until most of the free surface on the wall above the liquid level is covered.

Branched *fibre-like* crystals were seen to grow in the bulk liquid solution for all the three surfactants used in this study. Fig. 10 shows the presence of branched fibre-like crystal in the bulk liquid phase. The diameter of each fibre shown in the figure is approximately 1–2 μm. These fibre-like crystals were seen to grow at the same time when "mushy hydrate layer" (a term coined by Okutani et al. [5]) was also growing to cover the entire water/gas interface (Fig. 4). The growth of fibre-like crystals in the bulk water can also be seen in Fig. 11, where the red elliptical mark identifies the same crystal at the time indicated below each image. As seen, the red mark moves downwards in order to locate the same crystal because there is hydrate formation above it. This is due to the growth of crystal branches from the gas/liquid interface. The newly formed crystal is identified in Fig. 11d by a rectangle.

3.1. Mushy hydrate layer growth towards bulk water

Okutani et al. [5] reported that the mechanism of the downward growth of "mushy" hydrate layer into the bulk water is unclear at present and closer observations are required to study the mechanism. Based on our observation using a microscope (Fig. 12), the extent of the mushy hydrate layer in the bulk liquid solution increased due to the continuous hydrate formation on the base of the mushy hydrate layer (gas–liquid interface). There is also an animation given to illustrate how the mushy hydrate layer extends its length. Light blue triangle is an illustration of the mushy hydrate layer at 190 s and the dark blue color as the newly growth mushy hydrate layer at 10 s after the light blue triangle. The process of mushy hydrate layer growth towards the bulk water indicates that gas/water contact can be maintained through continuous water supply from the bulk to the interface. This requires that the mushy hydrate layer is porous to enable transfer of water from the bulk to the interface.

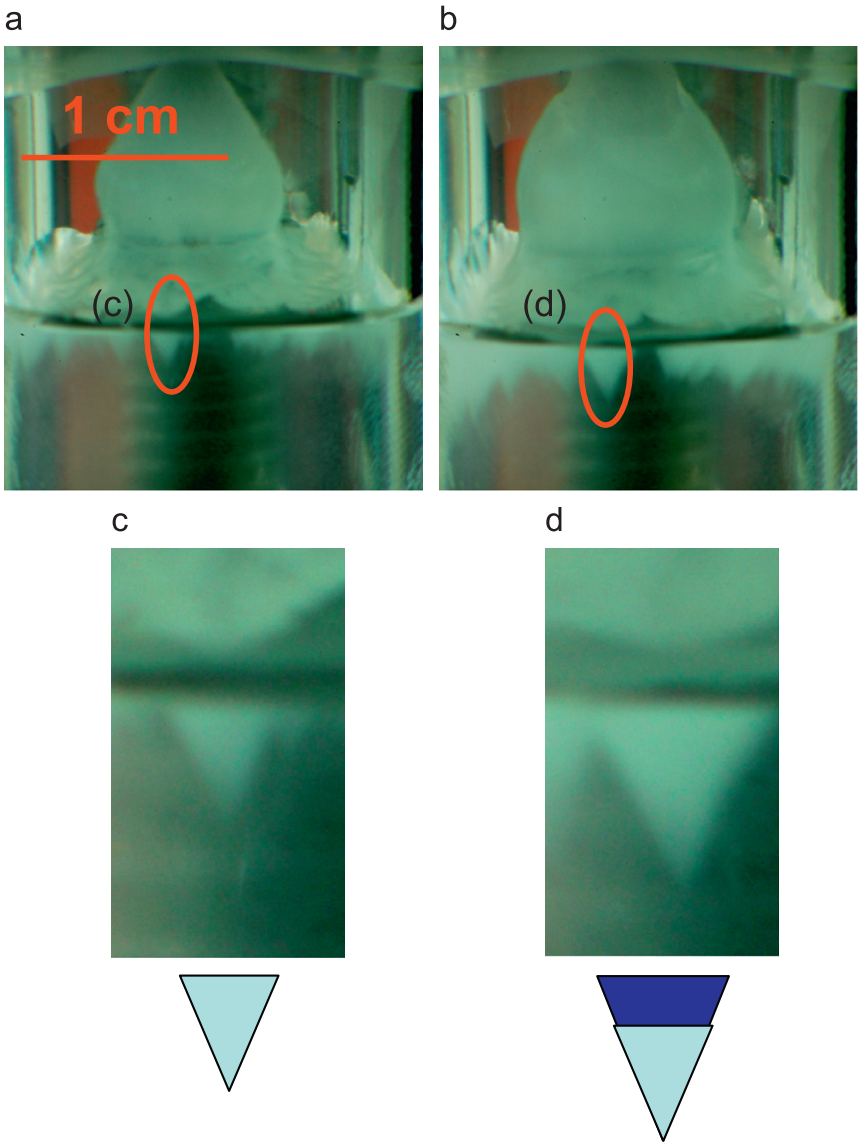

Fig. 12. Mechanism of mushy hydrate growth (Experiment G-2): (a) 190 sec, (b) 200 sec, (c) zoom of (c), and (d) zoom of (d).

3.2. Leaf-like crystal on the crystallizer wall

Two types of hydrate crystals were observed on the crystallizer wall (Fig. 13). A *leaf-like* crystal was seen to grow slowly. On the other side, a bulky hydrate was also seen attached to the wall, which was found to grow faster than the leaf-like crystals. Once, the bulky hydrate layer touches the leaf-like hydrate, water is seen travelling inside the leaf-like crystal structure. This phenomenon is shown in Fig. 14, where the color of the leaf-like crystal starts to change at the time when the bulky hydrate layer touches the leaf-like structure. At the same time the leaf-like hydrate crystal started to grow thicker possibly due to new water supply from the bulky hydrate layer. A less magnified view can be seen in the sequence of images in Fig. 15.

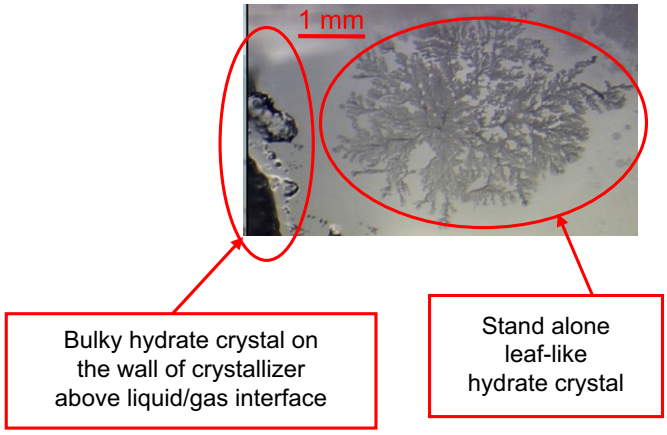

Fig. 13. Two different crystals (bulky-type and leaf-like) grow on the crystallizer wall (Experiment G-3).

3.3. Effect of surfactant concentration and undercooling

Many physical properties of liquid solutions, such as surface tension, are altered significantly when the surfactant concentration increases. Likewise, the hydrate formation rates are found to be affected by the SDS concentration. Our experiments with SDS at 3200 kPa, 2.4, and 13.1 K undercooling showed that the morphology of hydrate crystal growth was similar to the above described images with the degree of branching found to increase with increase in the concentration (Fig. 16). The degree of branching at 242 ppm is not shown but it was found to be similar to that for the SDS-645 ppm experiment.

Three experiments with different degrees of under-cooling (13.1, 8, and 3.6 K) were conducted with SDS and a concentration of 2200 ppm. It was found that at 13.1 and 8 K of under-cooling the hydrate crystal growth morphology was same but the extent of hydrate crystal formation was higher at 13.1 K. At the lowest degree of under-cooling there is no significant hydrate crystal growth but a thin hydrate layer on the crystallizer wall can still be seen.

4. Discussion

The above images illustrate that in the presence of the surfactant the growth of the hydrate crystals lack patterns like the dendrite crystals observed during hydrate formation in pure water.

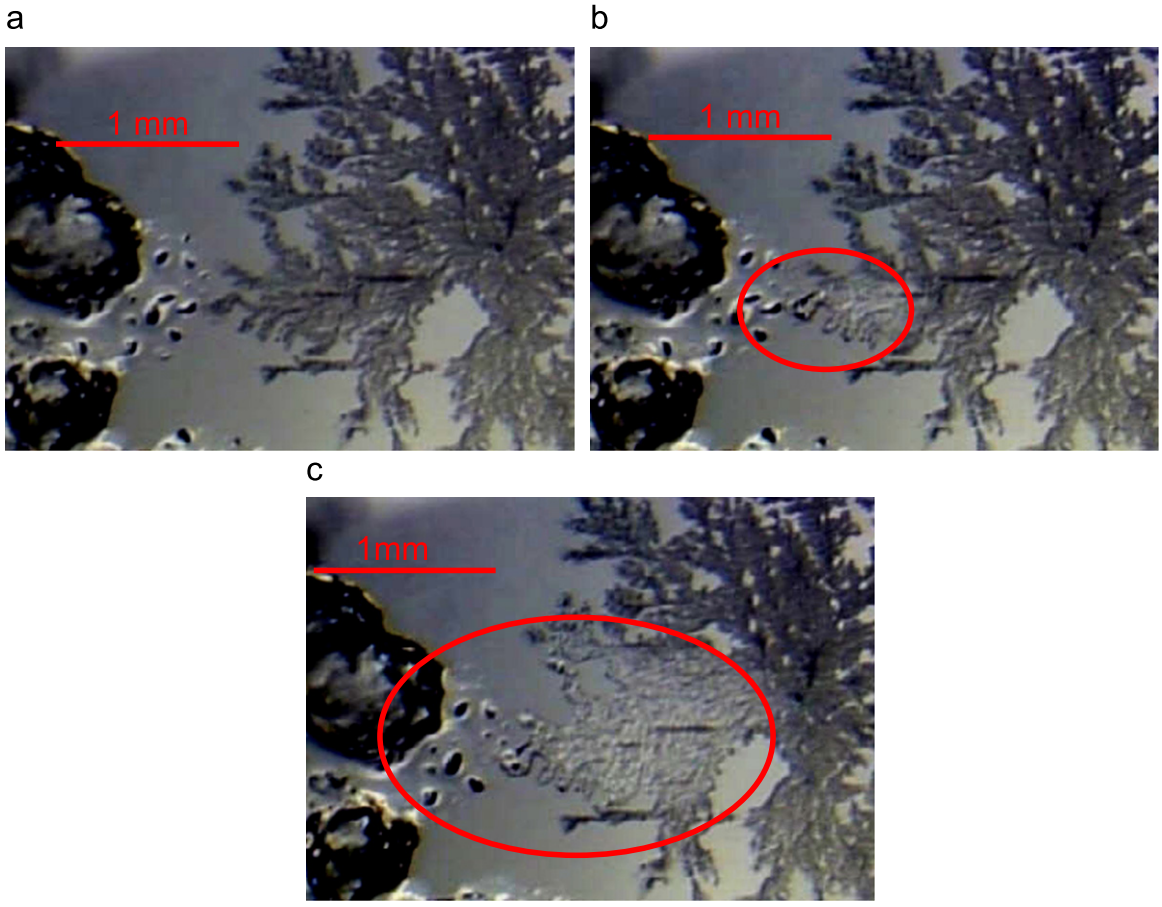

Fig. 14. Growth of leaf-like hydrate crystal at 13.1 K of under-cooling (Experiment G-3): (a) 3140 sec, (b) 3145 sec, and (c) 3160 sec.

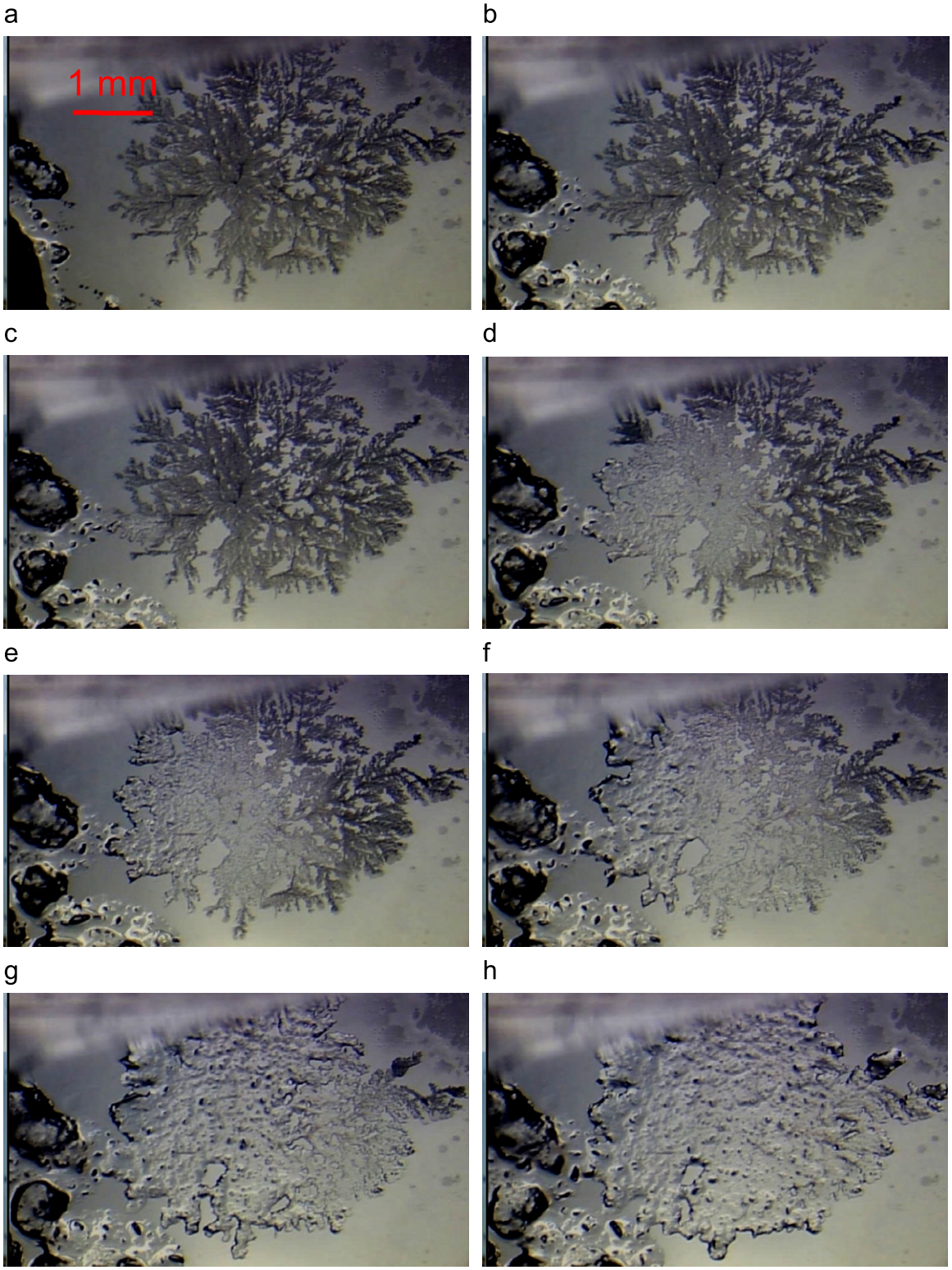

Fig. 15. Less magnified view of leaf-like crystal growth (Experiment G-3): (a) 2620 sec, (b) 3140 sec, (c) 3160 sec, (d) 3210 sec, (e) 3235 sec, (f) 3300 sec, (g) 3320 sec, and (h) 3400 sec.

Hydrate growth requires both water and gas and is sustained through the continuous contact of these phases. In addition, the rate depends on the degree of undercooling. In pure water the observed patterns are interpreted in terms of heat and mass transfer phenomena in the vicinity of a growing hydrate/water interface and well known phenomena such as the Mullins–Sekerka instability as was discussed extensively by Lee et al. [21] The observations reported in this work illustrate that the reproducible hydrate growth patterns (dendritic crystals) observed in pure water from the methane/propane (90.5/9.5 mol%) system at the under-cooling of 13.1 K and seen in Fig. 5 are not observed when surfactants are present. Kumar et al. [30] also reported that when

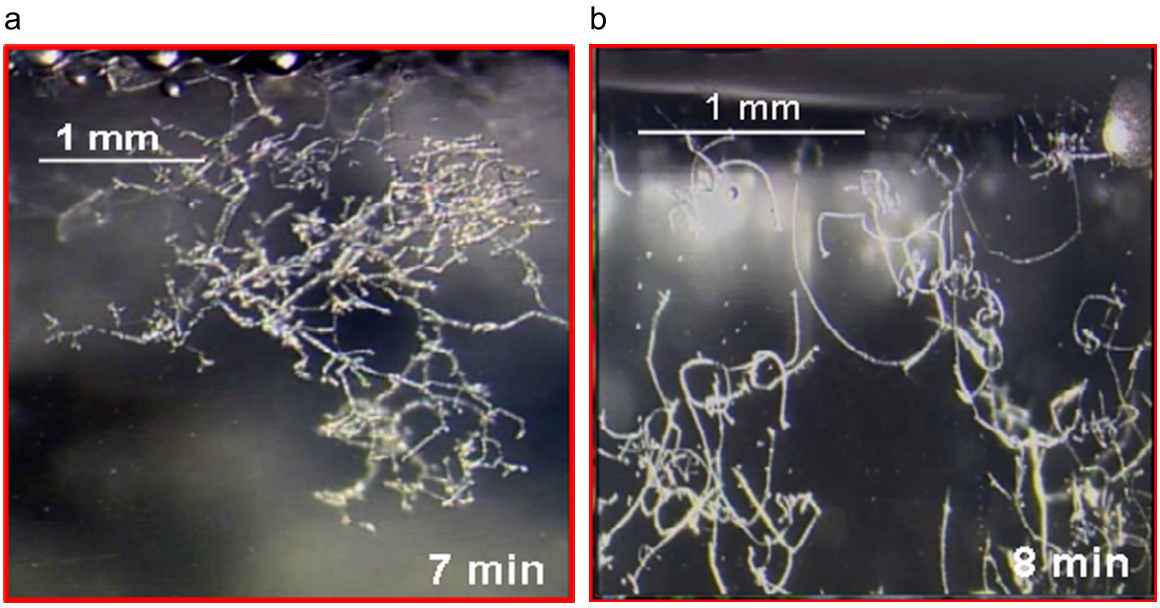

Fig. 16. . Hydrate crystal growth at different surfactant concentrations (Experiments B-1 and E-3). (a) Surfactant concentration of 2200 ppm (Experiment B-1) (b) surfactant concentration of 645 ppm (Experiment E-3).

small amount of 0.1 wt% PVP or poly(N-vinylpyrrolidone) was added to the water and contacted with methane/propane (90.5/9.5 mol%) gas mixture the hydrate crystals grown were not dendrites. It is noteworthy that the addition of the surfactant or PVP does not change the structure of the hydrate crystal. Structure II hydrate is formed in all cases.

In the presence of surfactants the growth observed is extensive and points to a situation, where the contact of water and gas is facilitated. The surfactant molecules are known to adsorb onto hydrate surfaces [15–18] and ice [31]. It is then plausible that in the vicinity of the surfactant molecule the growth of the hydrate crystal is "blocked" in a manner analogous to the well known action of hydrate kinetic inhibitors [36]. As a result in the case of a limited reactant (water or gas) the appearance of a leaf-like or a fibre-like crystal is seen, respectively. In the case of massive hydrate (at the gas/water interface) results in a voluminous hydrate that facilitates water transport (see mushy hydrate growth).

5. Conclusions

The dynamics of methane–propane hydrate crystal growth in solutions with or without the presence of surfactants (SDS, STS, and SHS) were studied. The surfactant concentrations used are 2200, 645, and 242 ppm for SDS, 300 ppm for STS, and 40 ppm for SHS. The conclusions are:

1. When surfactant is present in the system, hydrate formation no longer started to form as thin solid film at the liquid–gas interface but started on the crystallizer walls (gas–solid–liquid line) and formed thick, bulky layers, which grew upwards (along the crystallizer wall above gas–liquid interface) and then, followed by radial growth along the gas–liquid interface. This created a "mushy" hydrate layer that covered the gas–liquid interface and grew towards the bulk water.
2. Unlike the system with pure water, where needle-like dendrite crystals were found to grow from the gas–liquid interface to the bulk water, branches of fibre-like crystals were found to grow when surfactant is present in the system. It was also observed that increase in surfactant concentration increases branching of fibres compared to lower concentration.
3. The degree of under-cooling affects the extent of hydrate formation, where if ΔT increases, the extent of hydrate formation increases as expected.
4. Gas consumption was found to be approximately 14 times higher in the presence of surfactants compared to water for experiments conducted at the same driving force of 13.1 K.

Acknowledgements

We thank Natural Sciences and Engineering Research Council of Canada (NSERC) for the financial support.

References

[1] N. Kalogerakis, A.K.M. Jamaluddin, P.D. Dholabhai, P.R. Bishnoi, Effect of Surfactant on Hydrate Formation Kinetics, in: SPE International Symposium on Oilfield Chemistry, New Orleans 3/2-5/93, SPE25188, 1993, p. 375.
[2] J.S. Gudmundsson, V. Andersson, O.I. Levik, M. Parlaktuna, Hydrate Concept for Capturing Associated Gas, in: EUROPEC, SPE Paper 50598, the Hague, the Netherlands, 1998.
[3] J.S. Gudmundsson, V. Andersson, O.I. Levik, M. Mork, Hydrate Technology for Capturing Stranded Gas, in: Proceedings of Third International Conference on Gas Hydrates, Salt Lake City, 1999.
[4] J.S. Gudmundsson, O F. Graff, Hydrate Non-Pipeline Technology for Transport of Natural Gas, in: Proceedings of the 22nd World Gas Conference, Tokyo, Japan, 2003.
[5] K. Okutani, Y. Kuwabara, Y.H. Mori, Surfactant effects on hydrate formation in an unstirred gas/liquid system: an experimental study using methane and sodium alkyl sulfates, Chem. Eng. Sci. 63 (2008) 183–194.
[6] Y. Zhong, R.E. Rogers, Surfactant effects on gas hydrate formation, Chem. Eng. Sci. 55 (2000) 4175–4187.
[7] Y.H. Mori, Recent advances in hydrate based technologies for natural gas storage: a review, J. Chem. Ind. Eng. 54 (2003) 1–17.
[8] P. Englezos, J.D. Lee, Gas hydrates: a cleaner source of energy and opportunity for innovative technologies, Korean J. Chem. Eng. 22 (2005) 671–681.
[9] K. Watanabe, S. Imai, Y.H. Mori, Surfactant effects on hydrate formation in an unstirred gas/liquid system: an experimental study using HFC-32 and sodium dodecyl sulfate, Chem. Eng. Sci. 60 (2005) 4846–4857.
[10] U. Karaaslan, M. Parlaktuna, Surfactants as hydrate promoters?, Energy Fuels 14 (2000) 1103–1107.
[11] Z.-g. Sun, R. Wang, R. Ma, K. Guo, S. Fan, Natural gas storage in hydrates with the presence of promoters, Energy Convers. Manage. 44 (2003) 2733–2742.
[12] D.D. Link, E.P. Ladner, H.A. Elsen, C.E. Taylor, Formation and dissociation studies for optimizing the uptake of methane by methane hydrates, Fluid Phase Equilib. 211 (2003) 1–10.
[13] K. Okutani, Y. Kuwabara, Y.H. Mori, Surfactant effects on hydrate formation in an unstirred gas/liquid system: amendments to the previous study using HFC-32 and sodium dodecyl sulfate, Chem. Eng. Sci. 62 (2007) 3858–3860.

[14] T. Daimaru, A. Yamasaki, Y. Yanagisawa, Effect of surfactant carbon chain length on hydrate formation kinetics, J. Petrol Sci. Eng. 56 (2007) 89–96.
[15] J.S. Zhang, S. Lee, J.W. Lee, Does SDS micellize under methane hydrate-forming conditions below the normal Krafft point? J. Colloid Interface Sci. 315 (2007) 313–318.
[16] J.S. Zhang, C. Lo, P. Somasundaran, J.W. Lee, Competitive adsorption between SDS and carbonate on tetrahydrofuran hydrates, J. Colloid Interface Sci. 341 (2010) 286–288.
[17] J.S. Zhang, C. Lo, P. Somasundaran, S. Lu, A. Couzis, J.W. Lee, Adsorption of sodium dodecyl sulfate at THF hydrate/liquid interface, J. Phys. Chem. C 112 (2008) 12381–12385.
[18] C. Lo, J.S. Zhang, P. Somasundaran, S. Lu, A. Couzis, J.W. Lee, Adsorption of surfactants on two different hydrates, Langmuir 24 (2008) 12723–12726.
[19] O.B. Kutergin, V.P. Melnikov, A.N. Nesterov, Effect of surfacants on the mechanism and kinetics of hydrate formation of gases, Rep.Russ. Acad. Sci. 323 (N3) (1992) 349.
[20] P. Mel'nikov, A.N. Nesterov, V.V. Feklistov, Formation of gas hydrates in the presence of additives consisting of surface-active substances, Khimiia v Interesakh Ustoichivogo Razvitiia 6 (1998) 97–102.
[21] J.D. Lee, M. Song, R. Susilo, P. Englezos, Dynamics of methane–propane clathrate hydrate crystal growth from liquid water with or without the presence of n-heptane, Cryst. Growth Des. 6 (2006) 1428–1439.
[22] K. Watanabe, S. Niwa, Y.H. Mori, Surface tensions of aqueous solutions of sodium alkyl sulfates in contact with methane under hydrate-forming conditions, J. Chem. Eng. Data 50 (2005) 1672–1676.
[23] P. Gayet, C. Dicharry, G. Marion, A. Graciaa, J. Lachaise, A. Nesterov, Experimental determination of methane hydrate dissociation curve up to 55 MPa by using a small amount of surfactant as hydrate promoter, Chem. Eng. Sci. 60 (2005) 5751–5758.
[24] W.X. Pang, G.J. Chen, A. Dandekar, C.Y. Sun, C.L. Zhang, Experimental study on the scale-up effect of gas storage in the form of hydrate in a quiescent reactor, Chem. Eng. Sci. 62 (2007) 2198–2208.
[25] H. Tajima, F. Kiyono, A. Yamasaki, Direct observation of the effect of sodium dodecyl sulfate (SDS) on the gas hydrate formation process in a static mixer, Energy Fuels 24 (2010) 432–438.
[26] P. Servio, P. Englezos, Morphology study of structure H hydrate formation from water droplets, Cryst. Growth Des. 3 (2003) 61–66.
[27] P. Servio, P. Englezos, Morphology of methane and carbon dioxide hydrates formed from water droplets, AlChE J. 49 (2003) 269–276.
[28] M. Sugaya, Y.H. Mori, Behavior of clathrate hydrate formation at the boundary of liquid water and a fluorocarbon in liquid or vapor state, Chem. Eng. Sci. 51 (1996) 3505–3517.
[29] I. Kobayashi, Y. Ito, Y.H. Mori, Microscopic observations of clathrate–hydrate films formed at liquid/liquid interfaces. I. morphology of hydrate films, Chem. Eng. Sci. 56 (2001) 4331–4338.
[30] R. Kumar, J.D. Lee, M. Song, P. Englezos, Kinetic inhibitor effects on methane/propane clathrate hydrate-crystal growth at the gas/water and water/n-heptane interfaces, J. Cryst. Growth 310 (2008) 1154–1166.
[31] J. Yoslim, The effect of surfactant on the morphology of methane/propane clathrate hydrate crystals, Chemical and Biological Engineering, The University of British Columbia, Vancouver,, 2008.
[32] P. Di Profio, S. Arca, R. Germani, G. Savelli, Surfactant promoting effects on clathrate hydrate formation: are micelles really involved? Chem. Eng. Sci. 60 (2005) 4141–4145.
[33] W. Lin, G.J. Chen, C.Y. Sun, X.Q. Guo, Z.K. Wu, M.Y. Liang, L.T. Chen, L.Y. Yang, Effect of surfactant on the formation and dissociation kinetic behavior of methane hydrate, Chem. Eng. Sci. 59 (2004) 4449–4455.
[34] E.D. Sloan, Clathrate Hydrates of Natural Gases, Marcel Dekker, New York,, 1998.
[35] A.M. Kietzig, S.G. Hatzikiriakos, P. Englezos, Patterned superhydrophobic metallic surfaces, Langmuir 25 (2009) 4821–4827.
[36] B.J. Anderson, J.W. Tester, G.P. Borghi, B.L. Trout, Properties of inhibitors of methane hydrate formation via molecular dynamics simulations, J. Am. Chem. Soc. 127 (2005) 17852–17862.